

Extended Landauer-Büttiker Formula for Current through Open Quantum Systems with Gain or Loss

Chao Yang^{1,2,3} and Yucheng Wang^{1,2,3,*}

¹*Shenzhen Institute for Quantum Science and Engineering,
Southern University of Science and Technology, Shenzhen 518055, China*

²*International Quantum Academy, Shenzhen 518048, China*

³*Guangdong Provincial Key Laboratory of Quantum Science and Engineering,
Southern University of Science and Technology, Shenzhen 518055, China*

The Landauer-Büttiker formula, which characterizes the current flowing through a finite region connected to leads, has significantly advanced our understanding of transport. We extend this formula to describe particle and energy currents with gain or loss in the intermediate region by using the Lindblad-Keldysh formalism. Based on the derived formula, several novel effects induced by gain or loss in the current are discussed: the breaking of inversion symmetry in the gain and loss terms or in the system can lead to current generation; the anomalous phenomenon that disorder can induce current generation; the presence of gain and loss makes the thermal and electrical conductances continuous and ensures they follow the Wiedemann-Franz law even outside the energy band; the effect of bond loss-induced skin effect on current. This work deepens and extends our understanding of transport phenomena in open systems.

Introduction.— Studying electronic transport properties is essential for understanding condensed-matter systems and has broad applications, such as in various electronic devices, nanotechnology, and quantum computing [1–7]. One of the most influential frameworks for understanding transport in non-interacting mesoscopic systems is the Landauer-Büttiker formula [8, 9], which expresses the current in terms of the transmission coefficient of a system and the electron distribution within connected leads. The system described by this formula, aside from being coupled to two leads, is not influenced by any external environment.

Dissipation is widespread in various systems and profoundly impacts the dynamics of quantum systems. With the advancements in experimental techniques for controlling different types of dissipation [10–34], recent years have seen a growing interest in dissipative open quantum systems. While dissipation is typically viewed as detrimental to quantum correlations, recent research has revealed that it can also give rise to novel physical phenomena [13–26, 30–40] or phase transitions [41–52]. Understanding how dissipation affects quantum transport is a fundamentally important issue that has attracted wide attention in both theoretical and experimental research. A common type of dissipation is dephasing, which can significantly alter a system’s transport properties. For example, studies on its impact in disordered and quasiperiodic systems have shown that it can reduce coherence, thereby breaking localization and inducing diffusive transport [53–65]. Another common and important type of dissipation is particle gain or loss due to exchange between the system and the environment. In addition, experimental systems such as cold atomic systems and photonic quantum walk setups also provide a controlled way to study particle gains or losses [24–34]. The transport properties of a system with particle gain or

loss between two leads have inspired recent experimental and theoretical studies [26–34, 66–78], but there is still no general transport formula that is independent of the specific form of gain or loss, which has led to a less clear understanding of such systems compared to our understanding of the effect of dephasing dissipation on transport. To describe the transport properties of a system with gain or loss, what modifications and extensions are needed to the Landauer-Büttiker formula? What non-trivial transport properties can be revealed through the extended general formula? The motivation for this work is to answer these questions.

Model.— We consider a one-dimensional system with its ends coupled to leads, while also exchanging particles with reservoirs (see Fig. 1). The dynamics of the full system are described by the Lindblad equation [79, 80]

$$\frac{d\rho}{dt} = -i[H, \rho] + \sum_m (2L_m \rho L_m^\dagger - \{L_m^\dagger L_m, \rho\}), \quad (1)$$

with the Hamiltonian

$$H = H_S + \sum_{\alpha=L,R} (H_\alpha + H_{\alpha S}). \quad (2)$$

Here, $H_S = \sum_{ij} (\mathbf{h}_S)_{ij} c_i^\dagger c_j$ represents the Hamiltonian of the central system, where c_j is the annihilation operator at site j and $(\mathbf{h}_S)_{ij}$ is the i -th row and j -th column element of the matrix \mathbf{h}_S , representing the hopping amplitude between sites i and j . The subscripts $\alpha = L$ and $\alpha = R$ denote the left and right leads, respectively, with the corresponding Hamiltonian $H_\alpha = \sum_k \epsilon_{\alpha,k} d_{\alpha,k}^\dagger d_{\alpha,k}$, where $\epsilon_{\alpha,k}$ represents the energy of the k -th mode of the α -lead and $d_{\alpha,k}^\dagger$ ($d_{\alpha,k}$) is the creation (annihilation) operator for this mode. The term $H_{\alpha S} = \sum_{jk} t_{\alpha,kj} d_{\alpha,k}^\dagger c_j + h.c.$ describes the coupling between the α -lead and the central system, where $t_{\alpha,kj}$ is the corresponding tunneling

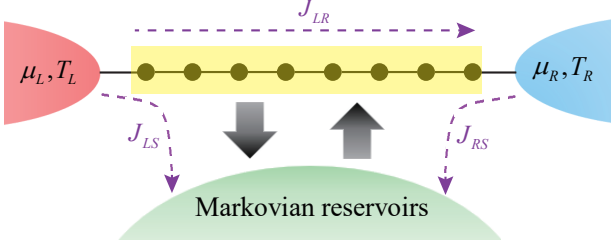


Figure 1: Model scheme: A central system (yellow region) is coupled to two leads at the left and right, with temperatures $T_{L(R)}$ and chemical potentials $\mu_{L(R)}$. The central system also connects to Markovian reservoirs (green region) for particle and energy transfer. The current through the system splits into three parts (Eq. (8)): J_{LR} , J_{LS} , and J_{RS} . J_{LR} is described by the Landauer-Büttiker formula, while the others arise from particle exchange with the reservoirs.

strength. The Lindblad operators L_m in Eq. (1) describe particle gain or loss in the central system as it exchanges particles with reservoirs. We assume linear coupling with

$$L_{1,i} = \sum_j u_{ij} c_j \quad \text{and} \quad L_{2,i} = \sum_j v_{ij} c_j^\dagger, \quad (3)$$

where $L_{1,i}$ and $L_{2,i}$ represent the loss and gain channels, respectively, which can be either on-site or non-local.

Generic formula.— We now derive the particle and energy currents for the above system, denoted as J^0 and J^1 , respectively. The particle (energy) currents flowing out of the left lead and into the right lead are, respectively, $J_L^0 = -\frac{dN_L}{dt}$ ($J_L^1 = -\frac{d\langle H_L \rangle}{dt}$) and $J_R^0 = \frac{dN_R}{dt}$ ($J_R^1 = \frac{d\langle H_R \rangle}{dt}$) [81], where $N_\alpha = \sum_k d_{\alpha,k}^\dagger d_{\alpha,k}$ and $\langle H_\alpha \rangle$ are the particle number and energy of the α -lead, respectively. Using $J_L^0 = -\frac{i}{\hbar} [H, N_L]$ and $J_L^1 = -\frac{i}{\hbar} [H, H_L]$, we can compute the currents flowing out of the left lead:

$$\begin{aligned} J_L^0 &= \frac{1}{\hbar} \sum_k (t_{L,kj} G_{SL,jk}^< - t_{L,kj}^* G_{LS,kj}^<), \\ J_L^1 &= \frac{1}{\hbar} \sum_k \epsilon_{L,k} (t_{L,kj} G_{SL,jk}^< - t_{L,kj}^* G_{LS,kj}^<). \end{aligned} \quad (4)$$

To trace out the leads, we use the Lindblad-Keldysh formalism [82–85]. The system's partition function can be written as $Z = \text{tr} \rho(t) = \int D[\bar{\psi}, \psi] e^{iS[\bar{\psi}, \psi]}$ [81], where S is the Keldysh action and $\psi = (\psi^+, \psi^-)$ are Grassmann variables defined on the upper and lower branches of the Keldysh contour. This description contains redundancy [82], and for computational convenience, a Keldysh rotation is often performed: $\psi^1 = \frac{1}{\sqrt{2}}(\psi^+ + \psi^-)$, $\psi^2 = \frac{1}{\sqrt{2}}(\psi^+ - \psi^-)$, $\bar{\psi}^1 = \frac{1}{\sqrt{2}}(\bar{\psi}^+ - \bar{\psi}^-)$, and $\bar{\psi}^2 = \frac{1}{\sqrt{2}}(\bar{\psi}^+ + \bar{\psi}^-)$. In this basis, the Keldysh action S of the central region can be rewritten as [81]

$$S = \int dt (\bar{\psi}^1 \quad \bar{\psi}^2) \begin{pmatrix} i\partial_t - \mathbf{X} & i\mathbf{Y} \\ 0 & i\partial_t - \mathbf{X}^\dagger \end{pmatrix} \begin{pmatrix} \psi^1 \\ \psi^2 \end{pmatrix}, \quad (5)$$

where $\mathbf{X} = \mathbf{h}_S - i\mathbf{P} - i\mathbf{Q}$ describes the damping dynamics [86, 87], and $\mathbf{Y} = 2(\mathbf{P} - \mathbf{Q})$ describes the imbalance between loss and gain. Note that the quantities in bold-face are matrices. The elements of the matrices \mathbf{P} and \mathbf{Q} are $P_{jk} = \sum_m u_{mj}^* u_{mk}$ and $Q_{jk} = \sum_m v_{mj} v_{mk}^*$, corresponding to the loss and gain terms, respectively. The system's retarded, advanced and Keldysh Green's functions are obtained by inverting the matrix (5): $\mathbf{g}_S^R = \frac{1}{\omega - \mathbf{X}}$, $\mathbf{g}_S^A = \frac{1}{\omega - \mathbf{X}^\dagger}$, $\mathbf{g}_S^K = -\frac{1}{\omega - \mathbf{X}} i\mathbf{Y} \frac{1}{\omega - \mathbf{X}^\dagger}$. Further combining the Langreth theorem [85, 88], after introducing the leads, one can obtain [81]:

$$\begin{aligned} \mathbf{G}_S^> &= i\mathbf{G}_S^R (f_L \Gamma_L + f_R \Gamma_R - \Gamma_L - \Gamma_R - 2\mathbf{P}) \mathbf{G}_S^A, \\ \mathbf{G}_S^< &= i\mathbf{G}_S^R (f_L \Gamma_L + f_R \Gamma_R + 2\mathbf{Q}) \mathbf{G}_S^A, \end{aligned} \quad (6)$$

where $f_\alpha = \frac{1}{e^{(\omega - \mu_\alpha)/k_B T_\alpha} + 1}$ is the Fermi distribution associated to the α -lead, $\mathbf{G}_S^R = (\mathbf{G}_S^A)^\dagger = [(\mathbf{g}_S^R)^{-1} - \tilde{\Sigma}_L^R - \tilde{\Sigma}_R^R]^{-1}$, and $\Gamma_\alpha = i(\tilde{\Sigma}_\alpha^R - \tilde{\Sigma}_\alpha^A)$ is the spectral density, with the lead self-energy being given by $\tilde{\Sigma}_\alpha^R = \Sigma_{S\alpha}^R \mathbf{g}_{\alpha S}^R$ ($\alpha \in \{L, R\}$). The Langreth theorem also provides the relationship between the full Green's function (\mathbf{G}) and the bare Green's function (\mathbf{g}):

$$\begin{aligned} \mathbf{G}_{LS}^< &= \mathbf{g}_L^< \Sigma_{LS}^A \mathbf{G}_S^A + \mathbf{g}_L^R \Sigma_{LS}^R \mathbf{G}_S^< + \mathbf{g}_L^< \Sigma_L^< \mathbf{G}_{LS}^A, \\ \mathbf{G}_{SL}^< &= \mathbf{G}_S^< \Sigma_{SL}^A \mathbf{g}_L^A + \mathbf{G}_S^R \Sigma_{SL}^R \mathbf{g}_L^< + \mathbf{G}_{SL}^R \Sigma_L^< \mathbf{g}_L^A. \end{aligned} \quad (7)$$

By substituting Eq. (7) into Eq. (4), the Green's functions of the system-lead coupling, \mathbf{G}_{LS} and \mathbf{G}_{SL} , can be replaced by the system Green's function, \mathbf{G}_S . Further applying Eq. (6), the current flowing out of the left lead, J_L^λ , can be derived (see Supplemental Material [81] for details), where $\lambda = 0$ and $\lambda = 1$ correspond to particle and energy currents, respectively. A similar procedure gives the current flowing into the right lead, J_R^λ . Due to the exchange of particles and energy between the central system and the environment, the currents flowing out of the left lead and into the right lead may differ, i.e., $J_L^\lambda \neq J_R^\lambda$ in the steady state. The total current through the system is given by $J^\lambda = \frac{1}{2}(J_L^\lambda + J_R^\lambda)$. These currents can be divided into three parts (see Fig. 1):

$$\begin{aligned} J^\lambda &= J_{LR}^\lambda + J_{LS}^\lambda - J_{RS}^\lambda, \\ J_{LR}^\lambda &= \int \frac{d\omega}{2\hbar} (f_L - f_R) \omega^\lambda \text{Tr}[\Gamma_L \mathbf{G}_S^R \Gamma_R \mathbf{G}_S^A + \Gamma_R \mathbf{G}_S^R \Gamma_L \mathbf{G}_S^A], \\ J_{L(R)S}^\lambda &= \int \frac{d\omega}{\hbar} f_{L(R)} \omega^\lambda \text{Tr}[\Gamma_{L(R)} \mathbf{G}_S^R \mathbf{P} \mathbf{G}_S^A] \\ &\quad + \int \frac{d\omega}{\hbar} (f_{L(R)} - 1) \omega^\lambda \text{Tr}[\Gamma_{L(R)} \mathbf{G}_S^R \mathbf{Q} \mathbf{G}_S^A]. \end{aligned} \quad (8)$$

The term J_{LR}^λ represents the Landauer-Büttiker formula, which describes the direct current between two leads. The total current through the system also includes $J_{LS}^\lambda - J_{RS}^\lambda$, representing the indirect current induced by the reservoirs. Here, $J_{L(R)S}$ consists of two parts: one describes the current from the leads to the loss channel through the central system, proportional to the particle

distribution $f_{L(R)}$, and the other describes the current from the gain channel to the leads through the central system, proportional to the hole distribution $1 - f_{L(R)}$.

Applications.— We will now discuss the interesting physical phenomena presented in Eq. (8). For convenience, the models we will discuss below as examples include only the nearest-neighbor hopping, i.e., $(\mathbf{h}_S)_{ij} = -t_S \delta_{i,j\pm 1}$, where t_S is the hopping strength, and unless otherwise specified, we set $t_S = 1$.

To directly observe the effects of gain and loss on the current from Eq. (8), we assume $f_L = f_R = f$, meaning there is no chemical potential ($\mu_L = \mu_R = \mu$) or temperature ($T_L = T_R = T$) difference between the two leads, resulting in no Landauer current J_{LR}^λ . From Eq. (8), we see that, under normal circumstances, gain and loss can generate a current. However, in two special cases, the current induced by gain and loss vanishes. The first case is when the gain and loss terms and the Fermi distribution satisfy $f\mathbf{P} + (f - 1)\mathbf{Q} = 0$, in this case, $J_{LS}^\lambda = J_{RS}^\lambda = 0$. In the low-energy limit $\omega \ll |\mu|, k_B T$, the condition for the current to vanish can be specifically written as $\frac{\mu}{k_B T} = \ln \frac{\mathbf{Q}}{\mathbf{P}}$. We consider that the added gain and loss terms in Eq. (3) are onsite with site-independent strength, namely: $L_{1,i} = \sqrt{\gamma_l} c_i$ and $L_{2,i} = \sqrt{\gamma_g} c_i^\dagger$. Fig. 2 (a) shows how the particle current J^0 changes with $\mu/k_B T$ and γ_g/γ_l . We observe that along the curve where $\gamma_g/\gamma_l = \mu/k_B T$, J^0 is zero, while on either side of this curve, J^0 is nonzero and opposite in direction.

The second case, in which the added gain and loss terms do not generate a current, is when the system and the gain and loss terms have center inversion symmetry, i.e., $\mathcal{P}^{-1} O_{ij} \mathcal{P} = O_{N-i+1, N-j+1}$, where the operator \mathbf{O} represents the Hamiltonian \mathbf{H} , the loss matrix \mathbf{P} , and the gain matrix \mathbf{Q} [89], and additionally, the spectral density matrix should satisfy $\mathcal{P}^{-1} \mathbf{\Gamma}_L \mathcal{P} = \mathbf{\Gamma}_R$. It is easy to show from Eq. (8) that in this case, $J_{LS}^\lambda = J_{RS}^\lambda$. In Fig. 2 (b1), we show an example of two sites with a local monitoring described by $L_{1,j} = \sqrt{\gamma_j} c_j$. In the limit $\gamma_j \ll \omega$, the current can be written analytically as [81]

$$J^0 \approx (\gamma_1 - \gamma_2) \Gamma \int \frac{d\omega}{h} f(\omega) \frac{|\omega + \frac{i\Gamma}{2}|^2 - 1}{|(\omega + \frac{i\Gamma}{2})^2 - 1|^2}, \quad (9)$$

where $\Gamma = (\mathbf{\Gamma}_L)_{11} = (\mathbf{\Gamma}_R)_{NN}$. From Eq. (9), we see that when $\gamma_1 = \gamma_2 = \gamma_0$, i.e., when both the system and the added loss exhibit the inversion symmetry, the current J^0 is always zero, regardless of γ_0 , as shown by the green line in Fig. 2 (b2). If the loss on one site is reduced to zero while the other remains at γ_0 , the inversion symmetry of the loss term is broken, and a current proportional to $\gamma_1 - \gamma_2$ is generated, as shown by the red and blue lines in Fig. 2(b2). Thus, when a system with inversion symmetry interacts with an environment, the environment induces particle or energy gain or loss. If the gain or loss term lacks inversion symmetry, a current will emerge, even if the strength of the gain or loss is

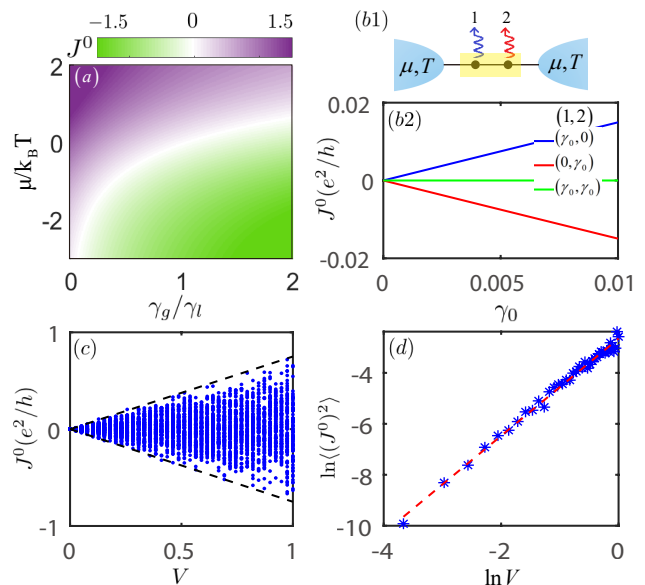


Figure 2: (a) J^0 as a function of γ_g/γ_l and $\mu/k_B T$, in units of e^2/h , with $k_B T = 20$, $\gamma_l = 0.2$, and the system size $N = 40$. (b1) Scheme of a two-site system with local monitoring. (b2) J^0 as a function of monitoring strength γ_0 . The blue and red curves represent monitoring at the first and second sites, respectively, while the green curve represents monitoring at both sites. (c) J^0 as a function of disorder strength V with 200 samples and $N = 100$. The black dashed line represents the envelope curve of the current. (d) The sample average of $(J^0)^2$. The red dashed line is the fitting function $\langle (J^0)^2 \rangle \sim V^{1.91}$. Other parameters are (b-d) $\mu = 0.1$, $k_B T = 10^{-4}$, $\gamma_l = 0.1$, and (a-d) $t_S = 1$, $(\mathbf{\Gamma}_L)_{11} = (\mathbf{\Gamma}_R)_{NN} = 1.1$.

weak. This property can be used to measure the characteristics of the environment.

On the other hand, if the gain and loss terms have inversion symmetry while the system itself does not, a current will also be generated. We consider that the added loss term is on-site, with the same strength at each site, so this term preserves inversion symmetry. The inversion symmetry of the system H_S is then broken by adding a disorder term $\sum_j V_j c_j^\dagger c_j$, where the on-site potential V_j is randomly distributed in $[-V, V]$. In one dimension, all the eigenstates are localized for arbitrarily small disorder strength V . Fig. 2(c) shows the current as a function of V . We see that when $V = 0$, $J^0 = 0$ as the system is inversion symmetric. As V increases, a finite current is observed. J^0 exhibits large fluctuations across samples. We further study the sample average of $(J^0)^2$, as shown in Fig. 2(d). We see that the sample-averaged $\langle (J^0)^2 \rangle$ follows a scaling relation with disorder strength: $\langle (J^0)^2 \rangle \sim V^2$ (see Supplemental Materials [81]). In a closed system, disorder obstructs particle transport. However, we observe that in an open system with gain or loss, disorder can cause the opposite effect, namely, it can lead to the generation of the current.

We then consider the current when there is a chemical

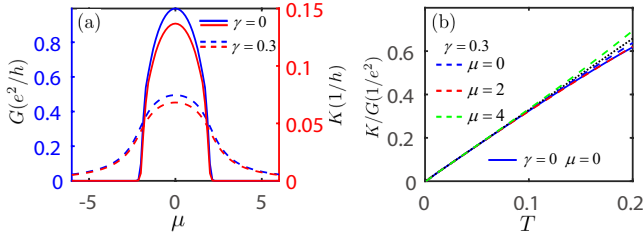


Figure 3: (a) G and K as functions of the chemical potential μ with temperature $T = 0.04$. (b) The ratio K/G as a function of T . $\mu = 0$, $\mu = 2$, and $\mu = 4$ are located inside the band, at the band edge, and outside the band, respectively. The black dotted line represents the Wiedemann-Franz law. Here we take $k_B = 1$, $t_S = 1$ and $N = 80$.

potential and temperature gradient between the leads, i.e., $f_L \neq f_R$. We set $\mu_R = \mu$, $T_R = T$, $f_R = f$, and $\mu_L = \mu + \delta\mu$, $T_L = T + \delta T$, $f_L = f + \delta f$. For convenience, we rewrite the current in Eq. (8) as two parts:

$$J^\lambda = J_0^\lambda + \delta J_1^\lambda, \quad (10)$$

where J_0^λ is the current when $\delta f = 0$, and δJ_1^λ is the current generated by $\delta f \neq 0$, which we refer to as the response current. From Eq. (8), it is easy to obtain

$$\delta J_1^\lambda = \int \frac{d\omega}{h} \omega^\lambda \delta f(\omega) \tau_1(\omega), \quad (11)$$

where $\tau_1(\omega) = \text{Tr}[\frac{1}{2}\mathbf{\Gamma}_L \mathbf{G}_S^R \mathbf{\Gamma}_R \mathbf{G}_S^A + \frac{1}{2}\mathbf{\Gamma}_R \mathbf{G}_S^R \mathbf{\Gamma}_L \mathbf{G}_S^A + \mathbf{\Gamma}_L \mathbf{G}_S^R (\mathbf{P} + \mathbf{Q}) \mathbf{G}_S^A]$ is the transmission function. We see that the effect of gain and loss on the response current manifests as the sum of the loss and gain matrices $(\mathbf{P} + \mathbf{Q})$. Additionally, all particles can contribute to the current J_0^λ if $f(\epsilon) \neq 0$, but only particles with energy ϵ within the energy window where $\delta f(\epsilon) \neq 0$ can contribute to the response current. Furthermore, δJ_1^λ can be related to $\delta\mu$ and δT through the Onsager matrix \mathbf{L} [63, 81, 90]:

$$\begin{pmatrix} \delta J_1^0 \\ \delta J_1^1 - \mu_L \delta J_1^0 \end{pmatrix} = \begin{pmatrix} L_{11} & L_{12} \\ L_{21} & L_{22} \end{pmatrix} \begin{pmatrix} \delta\mu/T \\ \delta T/T^2 \end{pmatrix}. \quad (12)$$

The electrical conductance is defined as $G = \frac{e^2}{T} L_{11}$ and the thermal conductance as $K = \frac{1}{T^2} \frac{\det|\mathbf{L}|}{L_{11}}$. In the low-temperature limit, the ratio of thermal to electrical conductance follows the Wiedemann-Franz law: $\frac{K}{G} \approx \mathcal{L}T$, with $\mathcal{L} = \frac{\pi^2}{3} (\frac{k_B}{e})^2$ being the Lorenz number.

In the absence of dissipation, both G and K are finite only within the energy band in the low-temperature limit, as shown by the blue and red solid lines in Fig. 3(a). Therefore, the Wiedemann-Franz law holds only within the band [Fig. 3(b)]. Then, we consider that each site of the system is subjected to equal loss and gain ($\gamma_l = \gamma_g = \gamma$), causing the conductances G and K to broaden and become smoother near the band edge, as indicated by the dashed lines in Fig. 3(a). As a result, the presence of

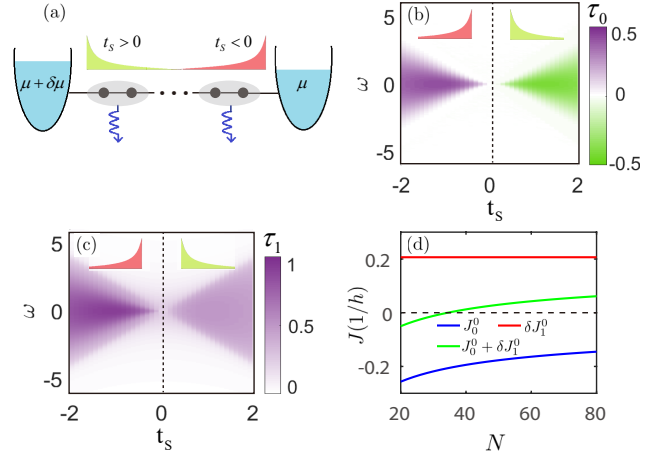


Figure 4: (a) Schematic of the setup to study transport in a system with skin effect caused by bond loss. The transmission functions (b) τ_0 and (c) τ_1 as a function of t_S and ω for a system with size $N = 80$. (d) The variation of J_0^0 , δJ_1^0 , and $J^0 = J_0^0 + \delta J_1^0$ with system size, with $t_S = 3$ fixed. Other parameters: (b-d) $\gamma_- = 1$, $\mu = 0.12$; (c-d) $\delta\mu = 0.6$.

gain and loss leads to the Wiedemann-Franz law holding both inside and outside the energy band, as shown by the dashed lines in Fig. 3(b).

Eq. (8) also applies to cases where the gain or loss is not on-site. As an example, we consider the bond-loss $L_j = \sqrt{\gamma_-}(c_j - ic_{j+1})$, which leads to the skin effect in the system: all the eigenstates are localized near the left (right) end for $t_S > 0$ ($t_S < 0$) [91, 92] [Fig. 4(a)]. In the zero-temperature limit, the current in Eq. (10) is given by $J_0^0 = \int_{-\infty}^{\mu} \frac{d\omega}{h} \tau_0(\omega)$ and $\delta J_1^0 = \int_{\mu}^{\mu+\delta\mu} \frac{d\omega}{h} \tau_1(\omega)$, where τ_0 and τ_1 are the transmission functions [81]. Figures 4(b) and (c) show τ_0 and τ_1 as functions of frequency ω and t_S , respectively. It can be seen that τ_0 is positive when all skin modes are localized at the right end and negative when they are localized at the left end. Since J_0^0 and τ_0 have the same sign, the current flows in the direction of the skin modes when $\mu_L = \mu_R$. Applying a voltage bias, i.e., $\delta\mu \neq 0$, generates the current δJ_1^0 , which always flows from high to low chemical potential, as shown in Fig. 4(c). Thus, if the voltage bias is applied at the opposite end from the skin modes, the direction of the total current depends on the competition between J_0^0 and δJ_1^0 . It can be shown that, in the thermodynamic limit, J_0^0 decreases with increasing system size and, for $|t_S| \geq |\gamma_-|$, satisfies: $J_0^0 \sim N^{-0.5}$ for $\mu \geq 0$ and $J_0^0 \sim \frac{e^{-N}}{N}$ for $\mu < 0$ [81]. This implies that the current corresponding to the skin mode vanishes as the system size tends to infinity, while δJ_1^0 does not depend on the system size [Fig. 4(d)]. Therefore, the direction of the current J^0 can be changed by altering the system size to change J_0^0 [Fig. 4(d)] or by changing $\delta\mu$ to adjust δJ_1^0 .

Conclusion.— We have derived a general formula for

the current through a region with particle exchange with the environment. This formula provides a new framework for studying the effects of particle gain or loss on transport properties. We have further demonstrated its usefulness by identifying novel transport features through several examples: (I) When the environmental influence on the particle's gain or loss lacks inversion symmetry, a current is generated; (II) When the gain or loss terms exhibit inversion symmetry, disorder can induce current generation; (III) The presence of gain and loss makes the transmission functions continuous and causes the ratio of thermal to electrical conductance at the band edges and in the gap to satisfy the Wiedemann-Franz law; (IV) The bond loss-induced skin effect and the current caused by the chemical potential difference exhibit an interesting competition. Further investigations are ongoing, and additional interesting phenomena and applications are anticipated to emerge.

This work is supported by National Key R&D Program of China under Grant No.2022YFA1405800, the Key-Area Research and Development Program of Guangdong Province (Grant No.2018B030326001), Guangdong Provincial Key Laboratory(Grant No.2019B121203002).

* Corresponding author: wangyc3@sustech.edu.cn

- [1] S. Datta, *Electronic Transport in Mesoscopic Systems*, (Cambridge University Press, 1997).
- [2] Y. Nazarov and Y. Blanter, *Quantum Transport: Introduction to Nanoscience*, (Cambridge University Press, 2009).
- [3] G. T. Landi, D. Poletti, and G. Schaller, Nonequilibrium boundary-driven quantum systems: Models, methods, and properties, *Rev. Mod. Phys.* **94**, 045006 (2022).
- [4] B. Bertini, F. Heidrich-Meisner, C. Karrasch, T. Prosen, R. Steinigeweg, and M. Žnidarič, Finite-temperature transport in one-dimensional quantum lattice models, *Rev. Mod. Phys.* **93**, 025003 (2021).
- [5] Y. Dubi and M. Di Ventra, Colloquium: Heat flow and thermoelectricity in atomic and molecular junctions, *Rev. Mod. Phys.* **83**, 131 (2011).
- [6] F. Verstraete, M. M. Wolf, and J. Ignacio Cirac, Quantum computation and quantum-state engineering driven by dissipation, *Nat. Phys.* **5**, 633 (2009).
- [7] A. Dhar, Heat transport in low-dimensional systems, *Advances in Physics* **57**, 457 (2008).
- [8] R. Landauer, Electrical resistance of disordered one-dimensional lattices, *Philos. Mag.* **21**, 863 (1970).
- [9] M. Büttiker, Four-Terminal Phase-Coherent Conductance, *Phys. Rev. Lett.* **57**, 1761 (1986).
- [10] H. Ritsch, P. Domokos, F. Brennecke, and T. Esslinger, Cold atoms in cavity-generated dynamical optical potentials, *Rev. Mod. Phys.* **85**, 553 (2013).
- [11] J. Barreiro, M. Müller, P. Schindler, D. Nigg, T. Monz, M. Chwalla, M. Hennrich, C. Roos, P. Zoller, and R. Blatt, An open-system quantum simulator with trapped ions, *Nature* **470**, 486 (2011).
- [12] H. Weimer, M. Müller, I. Lesanovsky, P. Zoller, and H. P. Büchler, A Rydberg quantum simulator, *Nat. Phys.* **6**, 382 (2010).
- [13] M. Müller, S. Diehl, G. Pupillo, and P. Zoller, Engineered open systems and quantum simulations with atoms and ions, *Advances in Atomic, Molecular, and Optical Physics* **61**, 1 (2012).
- [14] H. Krauter, C. A. Muschik, K. Jensen, W. Wasilewski, J. M. Petersen, J. I. Cirac, and E. S. Polzik, Entanglement Generated by Dissipation and Steady State Entanglement of Two Macroscopic Objects, *Phys. Rev. Lett.* **107**, 080503 (2011).
- [15] D. Kienzler, H.-Y. Lo, B. Keitch, L. de Clercq, F. Leupold, F. Lindenefelder, M. Marinelli, V. Negnevitsky, and J. P. Home, Quantum harmonic oscillator state synthesis by reservoir engineering, *Science* **347**, 53 (2015).
- [16] Z. Leghtas, S. Touzard, I. M. Pop, A. Kou, B. Vlastakis, A. Petrenko, K. M. Sliwa, A. Narla, S. Shankar, M. J. Hatridge, M. Reagor, L. Frunzio, R. J. Schoelkopf, M. Mirrahimi, and M. H. Devoret, Confining the state of light to a quantum manifold by engineered two-photon loss, *Science* **347**, 853 (2015).
- [17] P. M. Harrington, E. J. Mueller, and K. W. Murch, Engineered dissipation for quantum information science, *Nat. Rev. Phys.* **4**, 660 (2022).
- [18] S. Viciani, M. Lima, M. Bellini, and F. Caruso, Observation of Noise-Assisted Transport in an All-Optical Cavity-Based Network, *Phys. Rev. Lett.* **115**, 083601 (2015).
- [19] C. Maier, T. Brydges, P. Jurcevic, N. Trautmann, C. Hempel, B. P. Lanyon, P. Hauke, R. Blatt, and C. F. Roos, Environment-Assisted Quantum Transport in a 10-Qubit Network, *Phys. Rev. Lett.* **122**, 050501 (2019).
- [20] T. Tomita, S. Nakajima, I. Danshita, Y. Takasu, and Y. Takahashi, Observation of the Mott insulator to superfluid crossover of a driven-dissipative Bose-Hubbard system, *Science Advances* **3**, e1701513 (2017).
- [21] N. Dogra, M. Landini, K. Kroeger, L. Hruby, T. Donner, and T. Esslinger, Dissipation-induced structural instability and chiral dynamics in a quantum gas, *Science* **366**, 1496 (2019).
- [22] R. Bouganne, M. Bosch Aguilera, A. Ghermaoui, J. Beugnon, and F. Gerbier, Anomalous decay of coherence in a dissipative many-body system, *Nat. Phys.* **16**, 21 (2020).
- [23] D. Dreon, A. Baumgärtner, X. Li, S. Hertlein, T. Esslinger, and T. Donner, Self-oscillating pump in a topological dissipative atom-cavity system, *Nature* **608**, 494 (2022).
- [24] N. Syassen, D. M. Bauer, M. Lettner, T. Volz, D. Dietze, J. J. Garcia-Ripoll, J. I. Cirac, G. Rempe, and S. Dürr, Strong dissipation inhibits losses and induces correlations in cold molecular gases, *Science* **320**, 1329 (2008).
- [25] V. A. Brazhnyi, V. V. Konotop, V. M. Pérez-García, and H. Ott, Dissipation-induced coherent structures in Bose-Einstein condensates, *Phys. Rev. Lett.* **102**, 144101 (2009).
- [26] R. Labouvie, B. Santra, S. Heun, and H. Ott, Bistability in a driven-dissipative superfluid, *Phys. Rev. Lett.* **116**, 235302 (2016).
- [27] L. Corman, P. Fabritius, S. Häusler, J. Mohan, L. H. Dogra, D. Husmann, M. Lebrat, and T. Esslinger, Quantized conductance through a dissipative atomic point contact, *Phys. Rev. A* **100**, 053605 (2019).
- [28] M. Lebrat, S. Häusler, P. Fabritius, D. Husmann, L. Corman, and T. Esslinger, Quantized conductance through a

- spin-selective atomic point contact, *Phys. Rev. Lett.* **123**, 193605 (2019).
- [29] M.-Z. Huang, J. Mohan, A.-M. Visuri, P. Fabritius, M. Talebi, S. Wili, S. Uchino, T. Giamarchi, and T. Esslinger, Superfluid signatures in a dissipative quantum point contact, *Phys. Rev. Lett.* **130**, 200404 (2023).
- [30] R. El-Ganainy, K.G. Makris, M. Khajavikhan, Z.H. Musslimani, S. Rotter, and D.N. Christodoulides, Non-Hermitian physics and PT symmetry, *Nat. Phys.* **14**, 11(2018).
- [31] Ş. K. Özdemir, S. Rotter, F. Nori, and L. Yang, Parity-time symmetry and exceptional points in photonics, *Nat. Mater.* **18**, 783 (2019).
- [32] Y. Sun, T. Shi, Z. Liu, Z. Zhang, L. Xiao, S. Jia, and Y. Hu, Fractional Quantum Zeno Effect Emerging from Non-Hermitian Physics, *Phys. Rev. X* **13**, 031009 (2023).
- [33] L. Xiao, T. Deng, K. Wang, Z. Wang, W. Yi, and P. Xue, Observation of Non-Bloch Parity-Time Symmetry and Exceptional Points, *Phys. Rev. Lett.* **126**, 230402 (2021); P. Xue, Q. Lin, K. Wang, L. Xiao, S. Longhi, and W. Yi, Self acceleration from spectral geometry in dissipative quantum-walk dynamics, *Nat. Commun.* **15**, 4381 (2024); L. Xiao, W.-T. Xue, F. Song, Y.-M. Hu, W. Yi, Z. Wang, and P. Xue, Observation of Non-Hermitian Edge Burst in Quantum Dynamics, *Phys. Rev. Lett.* **133**, 070801 (2024).
- [34] J. Zhu, Y.-L. Mao, H. Chen, K.-X. Yang, L. Li, B. Yang, Z.-D. Li, and J. Fan, Observation of Non-Hermitian Edge Burst Effect in One-Dimensional Photonic Quantum Walk, *Phys. Rev. Lett.* **132**, 203801 (2024).
- [35] S. Diehl, A. Micheli, A. Kantian, B. Kraus, H. P. Büchler, and P. Zoller, Quantum states and phases in driven open quantum systems with cold atoms, *Nat. Phys.* **4**, 878 (2008); S. Diehl, A. Tomadin, A. Micheli, R. Fazio, and P. Zoller, Dynamical phase transitions and instabilities in open atomic many-body systems, *Phys. Rev. Lett.* **105**, 015702 (2010); S. Diehl, E. Rico, M. A. Baranov, and P. Zoller, Topology by dissipation in atomic quantum wires, *Nat. Phys.* **7**, 971 (2011).
- [36] F. Carollo, A. Lasanta, and I. Lesanovsky, Exponentially Accelerated Approach to Stationarity in Markovian Open Quantum Systems through the Mpemba Effect, *Phys. Rev. Lett.* **127**, 060401 (2021); A. K. Chatterjee, S. Takada, and H. Hayakawa, Quantum Mpemba Effect in a Quantum Dot with Reservoirs, *Phys. Rev. Lett.* **131**, 080402 (2023).
- [37] H.-P. Breuer, E.-M. Laine, J. Piilo, and B. Vacchini, Colloquium: Non-Markovian dynamics in open quantum systems, *Rev. Mod. Phys.* **88**, 021002 (2016); I. de Vega and D. Alonso, Dynamics of non-Markovian open quantum systems, *Rev. Mod. Phys.* **89**, 015001 (2017).
- [38] E. J. Bergholtz, J. C. Budich, and F. K. Kunst, Exceptional topology of non-Hermitian systems, *Rev. Mod. Phys.* **93**, 015005 (2021).
- [39] H. Weimer, A. Kshetrimayum, and R. Orús, Simulation methods for open quantum many-body systems, *Rev. Mod. Phys.* **93**, 015008 (2021).
- [40] M. Esposito, U. Harbola, and S. Mukamel, Nonequilibrium fluctuations, fluctuation theorems, and counting statistics in quantum systems, *Rev. Mod. Phys.* **81**, 1665 (2009).
- [41] T. Prosen and I. Pižorn, Quantum phase transition in a far-from-equilibrium steady state of an XY spin chain, *Phys. Rev. Lett.* **101**, 105701 (2008).
- [42] H. T. Mebrahtu, I. V. Borzenets, H. Zheng, Y. V. Bomze, A. I. Smirnov, S. Florens, H. U. Baranger, and G. Finkelstein, Observation of Majorana quantum critical behaviour in a resonant level coupled to a dissipative environment, *Nat. Phys.* **9**, 732 (2013); H. T. Mebrahtu, I. V. Borzenets, D. E. Liu, H. Zheng, Y. V. Bomze, A. I. Smirnov, H. U. Baranger, and G. Finkelstein, Quantum phase transition in a resonant level coupled to interacting leads, *Nature (London)* **488**, 61 (2012).
- [43] M. V. Medvedyeva, M. T. Čubrović, and S. Kehrein, Dissipation-induced first-order decoherence phase transition in a noninteracting fermionic system, *Phys. Rev. B* **91**, 205416 (2015).
- [44] K. Shastri and F. Monticone, Dissipation-induced topological transitions in continuous Weyl materials, *Phys. Rev. Res.* **2**, 033065 (2020).
- [45] M. Soriente, T. L. Heugel, K. Arimitsu, R. Chitra, and O. Zilberberg, Distinctive class of dissipation-induced phase transitions and their universal characteristics, *Phys. Rev. Res.* **3**, 023100 (2021).
- [46] W. Nie, M. Antezza, Y.-X. Liu, and F. Nori, Dissipative topological phase transition with strong system-environment coupling, *Phys. Rev. Lett.* **127**, 250402 (2021).
- [47] K. Yamamoto, M. Nakagawa, N. Tsuji, M. Ueda, and N. Kawakami, Collective excitations and nonequilibrium phase transition in dissipative fermionic superfluids, *Phys. Rev. Lett.* **127**, 055301 (2021).
- [48] K. Kawabata, T. Numasawa, and S. Ryu, Entanglement Phase Transition Induced by the Non-Hermitian Skin Effect, *Phys. Rev. X* **13**, 021007 (2023).
- [49] E. I. R. Chiacchio, A. Nunnenkamp, and M. Brunelli, Nonreciprocal Dicke Model, *Phys. Rev. Lett.* **131**, 113602 (2023).
- [50] Y. Liu, Z. Wang, C. Yang, J. Jie, and Y. Wang, Dissipation-induced extended-localized transition, *Phys. Rev. Lett.* **132**, 216301 (2024).
- [51] L.-N. Wu, J. Nettersheim, J. Feß, A. Schnell, S. Burgardt, S. Hiebel, D. Adam, A. Eckardt, and A. Widera, Indication of critical scaling in time during the relaxation of an open quantum system, *Nat. Commun.* **15**, 1714 (2024).
- [52] S. Longhi, Dephasing-induced mobility edges in quasicrystals, *Phys. Rev. Lett.* **132**, 236301 (2024).
- [53] S. A. Gurvitz, Delocalization in the Anderson Model due to a Local Measurement, *Phys. Rev. Lett.* **85**, 812 (2000).
- [54] A. G. Yamilov, R. Sarma, B. Redding, B. Payne, H. Noh, and H. Cao, Position-Dependent Diffusion of Light in Disordered Waveguides, *Phys. Rev. Lett.* **112**, 023904 (2014).
- [55] M. Balasubrahmaniam, S. Mondal, and S. Mujumdar, Necklace-State-Mediated Anomalous Enhancement of Transport in Anderson-Localized non-Hermitian Hybrid Systems, *Phys. Rev. Lett.* **124**, 123901 (2020).
- [56] S. Weidemann, M. Kremer, S. Longhi, and A. Szameit, Coexistence of dynamical delocalization and spectral localization through stochastic dissipation, *Nat. Photon.* **15**, 576 (2021).
- [57] M. V. Medvedyeva, T. Prosen, and M. Žnidarič, Influence of dephasing on many-body localization, *Phys. Rev. B* **93**, 094205 (2016).
- [58] E. Zerah-Harush and Y. Dubi, Effects of disorder and interactions in environment assisted quantum transport, *Phys. Rev. Res.* **2**, 023294 (2020).
- [59] S. Longhi, Anderson Localization in Dissipative Lattices, *Ann. Phys.* **535**, 2200658 (2023).
- [60] A. Purkayastha, A. Dhar, and M. Kulkarni, Nonequilibrium phase diagram of a one-dimensional quasiperiodic

- system with a single-particle mobility edge, *Phys. Rev. B* **96**, 180204(R) (2017).
- [61] M. Saha, B. P. Venkatesh, and B. K. Agarwalla, Quantum transport in quasiperiodic lattice systems in the presence of Büttiker probes, *Phys. Rev. B* **105**, 224204 (2022).
- [62] A. M. Lacerda, J. Goold, and G. T. Landi, Dephasing enhanced transport in boundary-driven quasiperiodic chains, *Phys. Rev. B* **104**, 174203 (2021).
- [63] C. Chiaracane, A. Purkayastha, M. T. Mitchison, and J. Goold, Dephasing-enhanced performance in quasiperiodic thermal machines, *Phys. Rev. B* **105**, 134203 (2022); C. Chiaracane, M. T. Mitchison, A. Purkayastha, G. Haack, and J. Goold, Quasiperiodic quantum heat engines with a mobility edge, *Phys. Rev. Res.* **2**, 013093 (2020).
- [64] D. Dwiputra and F. P. Zen, Environment-assisted quantum transport and mobility edges, *Phys. Rev. A* **104**, 022205 (2021).
- [65] V. Balachandran, S. R. Clark, J. Goold, and D. Poletti, Energy current rectification and mobility edges, *Phys. Rev. Lett.* **123**, 020603 (2019).
- [66] H. Fröml, A. Chiocchetta, C. Kollath, and S. Diehl, Fluctuation-Induced Quantum Zeno Effect, *Phys. Rev. Lett.* **122**, 040402 (2019).
- [67] M. Nakagawa, N. Tsuji, N. Kawakami, and M. Ueda, Dynamical Sign Reversal of Magnetic Correlations in Dissipative Hubbard Models, *Phys. Rev. Lett.* **124**, 147203 (2020).
- [68] T. Jin, M. Filippone, and T. Giamarchi, Generic transport formula for a system driven by Markovian reservoirs, *Phys. Rev. B* **102**, 205131 (2020).
- [69] D. Rossini, A. Ghermaoui, M.B. Aguilera, R. Vatré, R. Bouganne, J. Beugnon, F. Gerbier, and L. Mazza, Strong correlations in lossy one-dimensional quantum gases: From the quantum Zeno effect to the generalized Gibbs ensemble, *Phys. Rev. A* **103**, L060201 (2021).
- [70] T. Müller, M. Gievers, H. Fröml, S. Diehl, and A. Chiocchetta, Shape effects of localized losses in quantum wires: Dissipative resonances and nonequilibrium universality, *Phys. Rev. B* **104**, 155431 (2021).
- [71] V. Alba and F. Carollo, Noninteracting fermionic systems with localized losses: Exact results in the hydrodynamic limit, *Phys. Rev. B* **105**, 054303.
- [72] A.-M. Visuri, T. Giamarchi, and C. Kollath, Symmetry-Protected Transport through a Lattice with a Local Particle Loss, *Phys. Rev. Lett.* **129**, 056802 (2022); A.-M. Visuri, T. Giamarchi, and C. Kollath, Nonlinear transport in the presence of a local dissipation, *Phys. Rev. Res.* **5**, 013195 (2023).
- [73] A.-M. Visuri, J. Mohan, S. Uchino, M.-Z. Huang, T. Esslinger, and T. Giamarchi, DC transport in a dissipative superconducting quantum point contact, *Phys. Rev. Res.* **5**, 033095 (2023).
- [74] J. Ferreira, T. Jin, J. Mannhart, T. Giamarchi, and M. Filippone, *Phys. Rev. Lett.* **bf 132**, 136301 (2024).
- [75] G. Stefanucci, Kadanoff-Baym Equations for Interacting Systems with Dissipative Lindbladian Dynamics, *Phys. Rev. Lett.* **bf 133**, 066901 (2024).
- [76] K. Ganguly, M. Kulkarni, and B. K. Agarwalla, Transport in open quantum systems in presence of lossy channels, arXiv:2408.14399.
- [77] X. Cao, C. Jia, Y. Hu, and Z. Liang, Dissipative Nonlinear Thouless Pumping of Temporal Solitons, arXiv:2409.03450.
- [78] M.-Z. Huang, P. Fabritius, J. Mohan, M. Talebi, S. Wili, and T. Esslinger, Limited thermal and spin transport in a dissipative superfluid junction, arXiv:2412.08525.
- [79] G. Lindblad, On the generators of quantum dynamical semigroups, *Commun. Math. Phys.* **48**, 119 (1976).
- [80] H.-P. Breuer and F. Petruccione, *The Theory of Open Quantum Systems* (Oxford University Press, Oxford, 2002).
- [81] See Supplemental Material for details on (I) definition of particle and energy currents; (II) Keldysh theory of open fermionic systems; (III) deriving the extended Landauer-Büttiker formula; (IV) effect of inversion symmetry in gain or loss terms on the current; (V) disorder-induced current generation; (VI) response current and the Wiedemann-Franz law; and (VII) J_0^0 variation with size in the presence of skin effect. The Supplemental Materials includes the references [63, 82, 90, 93–97].
- [82] L. M. Sieberer, M. Buchhold, and S. Diehl, Keldysh field theory for driven open quantum systems, *Rep. Prog. Phys.* **79**, 096001 (2016).
- [83] A. Kamenev, *Field Theory of Non-Equilibrium Systems* (Cambridge University Press, Cambridge, 2011).
- [84] A. Altland and B. Simons, *Condensed Matter Field Theory* (Cambridge University Press, Cambridge, 2006).
- [85] H. J. W. Haug and A.-P. Jauho, *Quantum Kinetics in Transport and Optics of Semiconductors* (Springer, 2008).
- [86] T. Prosen, Third quantization: a general method to solve master equations for quadratic open Fermi systems, *New J. Phys.* **10** 043026 (2008).
- [87] C. E. Bardyn, M. A. Baranov, C. V. Kraus, E. Rico, A. Imamoglu, P. Zoller and S. Diehl, Topology by dissipation, *New J. Phys.* **15** 085001 (2013).
- [88] D. C. Langreth, in *Linear and Nonlinear Electron Transport in Solids*, edited by J. T. Devreese and V. E. VanDoren (Plenum, New York, 1976).
- [89] It is easy to prove that when the Hamiltonian \mathbf{H} , the loss matrix \mathbf{P} , and the gain matrix \mathbf{Q} satisfy inversion symmetry, \mathbf{G}_S^R and \mathbf{G}_S^A also satisfy inversion symmetry. Therefore, \mathbf{O} also corresponds to \mathbf{G}_S^R and \mathbf{G}_S^A .
- [90] P. N. Butcher, Thermal and electrical transport formalism for electronic microstructures with many terminals, *J. Phys.: Condens. Matter* **2**, 4869 (1990).
- [91] F. Song, S. Yao, and Z. Wang, Non-Hermitian Skin Effect and Chiral Damping in Open Quantum Systems, *Phys. Rev. Lett.* **123**, 170401 (2019).
- [92] C.-H. Liu, K. Zhang, Z. Yang, and S. Chen, Helical damping and dynamical critical skin effect in open quantum systems, *Phys. Rev. Research* **2**, 043167 (2020).
- [93] K. Yamamoto, N. Hatano, Thermodynamics of the mesoscopic thermoelectric heat engine beyond the linear-response regime, *Phys. Rev. E* **92**, 042165 (2015).
- [94] F. Thompson, A. Kamenev, Field theory of many-body Lindbladian dynamics, *Annals of Physics*, **455**, 169385 (2023).
- [95] Y. Meir, N. S. Wingreen, Landauer formula for the current through an interacting electron region, *Phys. Rev. Lett.* **68**, 2512 (1992).
- [96] D. A. Lavis, B. W. Southern, The inverse of a symmetric banded toeplitz matrix, *Rep. Math. Phys.* **39**, 137 (1997).
- [97] M. Saha, B. K. Agarwalla, M. Kulkarni, A. Purkayastha, Universal Subdiffusive Behavior at Band Edges from Transfer Matrix Exceptional Points, *Phys. Rev. Lett.* **130**, 187101 (2023).

Supplementary Material: Extended Landauer-Büttiker Formula for Current through Open Quantum Systems with Gain or Loss

In the Supplementary Materials, we first provide the definition of the current, then introduce the Keldysh theory of open fermionic systems, and present the derivation details of the extended Landauer-Büttiker formula. Next, we analytically analyze the effect of inversion symmetry in gain or loss terms on the current using a two-site model, and examine how disorder-induced symmetry breaking leads to the generation of current. Finally, we study the impact of gain or loss on the Wiedemann-Franz law and investigate the behavior of the current in the presence of the skin effect.

I. Definition of particle and energy currents

The steady state of the system we study (Fig. 1 in the main text) is not in equilibrium, which leads to difficulties in defining the global thermodynamic variables. To overcome this problem, it is convenient to instead study the particle and energy flows in the lead [S1]. From the first law of thermodynamics, we have

$$dU_{L(R)} = dQ_{L(R)} + dW_{L(R)}, \quad (\text{S1})$$

where $U_{L(R)} = \langle H_{L(R)} \rangle$ is the energy of $L(R)$ -lead, $dU_{L(R)}$ and $dQ_{L(R)}$ are the energy and heat flowing into the $L(R)$ -lead, and $dW_{L(R)} = \mu_{L(R)} d\mathcal{N}_{L(R)}$, with $\mathcal{N}_{L(R)}$ being the particle number of the $L(R)$ -lead, is the work done on the $L(R)$ -lead. Typically, the voltage V is defined as the difference of chemical potential, $eV = \mu_R - \mu_L$. The particle and energy currents are then defined as

$$J_L^0 = -\frac{d\mathcal{N}_L}{dt}, \quad J_R^0 = \frac{d\mathcal{N}_R}{dt}, \quad J_L^1 = -\frac{dU_L}{dt}, \quad J_R^1 = \frac{dU_R}{dt}. \quad (\text{S2})$$

Substituting into Eq. (S1), we see that the heat current is

$$J_L^Q = -\frac{dQ_L}{dt} = J_L^1 - \mu_L J_L^0, \quad J_R^Q = \frac{dQ_R}{dt} = J_R^1 - \mu_R J_R^0. \quad (\text{S3})$$

It is common to study the net current J defined by

$$J^{0/1/Q} = \frac{1}{2}(J_L^{0/1/Q} + J_R^{0/1/Q}). \quad (\text{S4})$$

II. Keldysh theory of open fermionic systems

In a system coupled with the environment, one often studies the reduced density matrix ρ . Under the Markovian approximation, the evolution of ρ can be described by the Lindblad master equation

$$\frac{d\rho}{dt} = -i[H, \rho] + \sum_m (2L_m \rho L_m^\dagger - \{L_m^\dagger L_m, \rho\}). \quad (\text{S5})$$

Here, H is the Hamiltonian (renormalized by the environment), and L_m are the quantum jump operators describing the coupling between the system and the environment. It is convenient to introduce the Lindblad-Keldysh partition function, $Z = \text{Tr}[\rho(t)]$, which is always equal to one due to the normalization of the density matrix. By inserting fermionic coherent states $|\psi\rangle$, which are eigenstates of the annihilation operators: $c_j|\psi\rangle = \psi_j|\psi\rangle$, the partition function can be written as $Z = \int D[\bar{\psi}^\pm, \psi^\pm] e^{i\mathcal{S}}$ [S2, S3], where the superscript \pm denotes the indices of Keldysh contour, and the action reads

$$\mathcal{S} = \int dt \left[\sum_j (\bar{\psi}_j^+ i\partial_t \psi_j^+ - \bar{\psi}_j^- i\partial_t \psi_j^-) - i\mathcal{L} \right]. \quad (\text{S6})$$

Here, the Liouvillian $\mathcal{L} = -iH^+ + iH^- - (L^\dagger L)^+ - (L^\dagger L)^- + 2(L)^+(L^\dagger)^-$, where H^\pm and L^\pm satisfy: $O^+ = \frac{\langle \psi^+(t_{n+1}) | O | \psi^+(t_n) \rangle}{\langle \psi^+(t_{n+1}) | \psi^+(t_n) \rangle}$ and $O^- = \frac{\langle -\psi^-(t_n) | O | -\psi^-(t_{n+1}) \rangle}{\langle -\psi^-(t_n) | -\psi^-(t_{n+1}) \rangle}$, with O representing H or L . The description in this basis often contains redundancy. To eliminate this redundancy and facilitate calculations, a Keldysh rotation is usually performed,

$$\begin{cases} \psi^1 = \frac{1}{\sqrt{2}}(\psi^+ + \psi^-), \\ \psi^2 = \frac{1}{\sqrt{2}}(\psi^+ - \psi^-). \end{cases} \quad \begin{cases} \bar{\psi}^1 = \frac{1}{\sqrt{2}}(\bar{\psi}^+ - \bar{\psi}^-), \\ \bar{\psi}^2 = \frac{1}{\sqrt{2}}(\bar{\psi}^+ + \bar{\psi}^-). \end{cases} \quad (\text{S7})$$

Hence, the Liouvillian and action can be expressed as functions of $\bar{\psi}^{1,2}$ and $\psi^{1,2}$.

Suppose the Hamiltonian is non-interacting and the Lindbladian is linear,

$$H = \sum_{jk} h_{jk} c_j^\dagger c_k, \quad L_{1,j} = \sum_k u_{jk} c_k, \quad L_{2,j} = \sum_k v_{jk} c_k^\dagger. \quad (\text{S8})$$

The action is quadratic and can be written in matrix form in Keldysh space:

$$S = \int dt \begin{pmatrix} \bar{\psi}^1 & \bar{\psi}^2 \end{pmatrix} \begin{pmatrix} i\partial_t - \mathbf{h} + i\mathbf{P} + i\mathbf{Q} & -2i(\mathbf{Q} - \mathbf{P}) \\ 0 & i\partial_t - \mathbf{h} - i\mathbf{P} - i\mathbf{Q} \end{pmatrix} \begin{pmatrix} \psi^1 \\ \psi^2 \end{pmatrix}, \quad (\text{S9})$$

where the matrix element of the loss matrix \mathbf{P} is $P_{jk} = \sum_m u_{mj}^* u_{mk}$, and the matrix element of the gain matrix \mathbf{Q} is $Q_{jk} = \sum_m v_{mj} v_{mk}^*$. It is convenient to define the damping matrix $\mathbf{X} = \mathbf{h} - i\mathbf{P} - i\mathbf{Q}$ and the imbalance matrix $\mathbf{Y} = 2(\mathbf{P} - \mathbf{Q})$. The Green's functions can be derived by inverting the action matrix \mathbf{S} , i.e.,

$$\begin{pmatrix} \mathbf{g}_{jk}^{\mathcal{R}} & \mathbf{g}_{jk}^{\mathcal{K}} \\ 0 & \mathbf{g}_{jk}^{\mathcal{A}} \end{pmatrix} = \begin{pmatrix} i\partial_t - \mathbf{X} & i\mathbf{Y} \\ 0 & i\partial_t - \mathbf{X}^\dagger \end{pmatrix}^{-1}. \quad (\text{S10})$$

If we focus on the steady state, the Green's function depends only on the time difference $t - t'$. Hence, the explicit expressions of the Green's functions in the frequency domain are

$$\mathbf{g}^{\mathcal{R}} = \frac{1}{\omega - \mathbf{X}}, \quad \mathbf{g}^{\mathcal{A}} = \frac{1}{\omega - \mathbf{X}^\dagger}, \quad \mathbf{g}^{\mathcal{K}} = -\frac{1}{\omega - \mathbf{X}} i\mathbf{Y} \frac{1}{\omega - \mathbf{X}^\dagger}. \quad (\text{S11})$$

We see that the retarded and advanced Green's functions contain only the spectral information of the damping matrix, while the Keldysh Green's function, which captures the particle distribution in the steady state, contains both the spectral information of \mathbf{X} and the imbalance matrix \mathbf{Y} . By using the identities $\mathbf{g}^> = \frac{1}{2}(\mathbf{g}^{\mathcal{K}} + \mathbf{g}^{\mathcal{R}} - \mathbf{g}^{\mathcal{A}})$ and $\mathbf{g}^< = \frac{1}{2}(\mathbf{g}^{\mathcal{K}} - \mathbf{g}^{\mathcal{R}} + \mathbf{g}^{\mathcal{A}})$, the steady-state greater and lesser Green's functions can be derived

$$\mathbf{g}^> = -2i\mathbf{g}^{\mathcal{R}}\mathbf{P}\mathbf{g}^{\mathcal{A}}, \quad \mathbf{g}^< = 2i\mathbf{g}^{\mathcal{R}}\mathbf{Q}\mathbf{g}^{\mathcal{A}}. \quad (\text{S12})$$

We can see that the greater Green's function is directly proportional to the loss matrix \mathbf{P} and the lesser Green's function is directly proportional to the gain matrix \mathbf{Q} .

III. Derivation details of extended Landauer-Büttiker formula

Suppose the full Hamiltonian of the system shown in Fig. 1 of the main text is

$$H = H_S + H_L + H_R + (H_{SL} + H_{SR} + h.c.), \quad (\text{S13})$$

where H_S is the Hamiltonian of the central system, $H_{L(R)}$ are the Hamiltonians of left (right) leads, and $H_{SL(SR)}$ represents the coupling between the central system and the left (right) lead. We assume that the Markovian reservoirs only interact with the central system, and hence the Lindblad operators L_m contain only the operators acting on the central system. The explicit form of the Hamiltonian in Eq. (S13) is

$$\begin{aligned} H_S &= \sum_{ij} h_{S,ij} c_i^\dagger c_j, & H_L &= \sum_k \epsilon_{L,k} d_{L,k}^\dagger d_{L,k}, & H_R &= \sum_k \epsilon_{R,k} d_{R,k}^\dagger d_{R,k}, \\ H_{LS} &= \sum_{kj} t_{L,kj} d_{L,k}^\dagger c_j, & H_{RS} &= \sum_{kj} t_{R,kj} d_{R,k}^\dagger c_j. \end{aligned} \quad (\text{S14})$$

Here $c_j(c_j^\dagger)$ is the annihilation (creation) operator on the j -th lattice site of the central system, and $d_{L(R),k}(d_{L(R),k}^\dagger)$ is the annihilation (creation) operator on the momentum k of the left (right) lead. We first consider the current flowing out of the left lead, as shown in Eq. (S2), which can be calculated by

$$\begin{aligned} J_L^0 &= -\frac{d\mathcal{N}_L}{dt} = -\frac{i}{\hbar}[H, \mathcal{N}_L] = \frac{1}{\hbar} \sum_k (t_{L,kj} G_{SL,jk}^< - t_{L,kj}^* G_{LS,kj}^<), \\ J_L^1 &= -\frac{dU_L}{dt} = -\frac{i}{\hbar}[H, U_L] = \frac{1}{\hbar} \sum_k \epsilon_{L,k} (t_{L,kj} G_{SL,jk}^< - t_{L,kj}^* G_{LS,kj}^<), \end{aligned} \quad (\text{S15})$$

Here, the particle number operator is $\mathcal{N}_L = \sum_k d_{L,k}^\dagger d_{L,k}$ and the energy is $U_L = \sum_k \epsilon_{L,k} d_{L,k}^\dagger d_{L,k}$. To derive this equation, we used the Heisenberg equation of motion for operators, which is valid here because the leads are assumed to be uncoupled from the reservoir. In a more general scenario where the reservoir is coupled to both the central system and the leads, one would instead use the Lindblad equation for operators. In the following, we use \mathbf{g} to denote the bare Green's function (i.e., the Green's function without coupling to the leads), and \mathbf{G} to denote the full Green's functions. By applying the Langreth theorem, one can obtain

$$\begin{aligned} \mathbf{G}_{LS}^< &= \mathbf{g}_L^< \Sigma_{LS}^A \mathbf{G}_S^A + \mathbf{g}_L^R \Sigma_{LS}^R \mathbf{G}_S^< + \mathbf{g}_L^R \Sigma_L^< \mathbf{G}_{LS}^A, \\ \mathbf{G}_{SL}^< &= \mathbf{G}_S^< \Sigma_{SL}^A \mathbf{g}_L^A + \mathbf{G}_S^R \Sigma_{SL}^R \mathbf{g}_L^< + \mathbf{G}_{SL}^R \Sigma_L^< \mathbf{g}_L^A. \end{aligned} \quad (\text{S16})$$

and

$$\begin{aligned} \mathbf{G}_S^< &= \mathbf{g}_S^< + (\mathbf{g}_S^< \Sigma_{SL}^A \mathbf{G}_{LS}^A + \mathbf{g}_S^R \Sigma_{SL}^R \mathbf{G}_{LS}^< + \mathbf{g}_S^R \Sigma_{SL}^< \mathbf{G}_{LS}^A + L \leftrightarrow R), \\ \mathbf{G}_S^> &= \mathbf{g}_S^> + (\mathbf{g}_S^> \Sigma_{SL}^A \mathbf{G}_{LS}^A + \mathbf{g}_S^R \Sigma_{SL}^R \mathbf{G}_{LS}^> + \mathbf{g}_S^R \Sigma_{SL}^> \mathbf{G}_{LS}^A + L \leftrightarrow R). \end{aligned} \quad (\text{S17})$$

Here, $\Sigma_L^<$ vanishes for non-interacting, non-dissipating leads. In equilibrium, the bare Green's functions of the left lead are

$$g_{L,k}^< = 2\pi i f_L \delta(\omega - \epsilon_{L,k}), \quad g_{L,k}^> = 2\pi i (f_L - 1) \delta(\omega - \epsilon_{L,k}), \quad (\text{S18})$$

where $f_L = \frac{1}{e^{(\omega - \mu_L)/k_B T_L} + 1}$ is the Fermi distribution. Transforming into the frequency domain, $G(t - t') = \int \frac{d\omega}{2\pi} e^{-i\frac{\omega(t-t')}{\hbar}} G(\omega)$, and substituting Eq. (S16) and (S18) into Eq. (S15), we get

$$J_L^\lambda = \frac{i}{\hbar} \int \frac{d\omega}{2\pi} \omega^\lambda \text{Tr} [f_L \mathbf{\Gamma}_L (\mathbf{G}_S^R - \mathbf{G}_S^A) + \mathbf{\Gamma}_L \mathbf{G}_S^<]. \quad (\text{S19})$$

Here, $\lambda = 0, 1$, and the spectral density is $\mathbf{\Gamma}_L = i(\tilde{\Sigma}_L^R - \tilde{\Sigma}_L^A)$, with the leads-induced self-energies $\tilde{\Sigma}_L^R = \Sigma_{SL}^R \mathbf{g}_L^R \Sigma_{LS}^R$, and $\tilde{\Sigma}_L^A = \Sigma_{SL}^A \mathbf{g}_L^A \Sigma_{LS}^A$. The expression for J_R^λ can be derived in the same way. Substituting J_L^λ and J_R^λ into Eq. (S4), the current J^λ can be written as

$$J^\lambda = \frac{i}{2\hbar} \int \frac{d\omega}{2\pi} \omega^\lambda \text{Tr} [(f_L \mathbf{\Gamma}_L - f_R \mathbf{\Gamma}_R) (\mathbf{G}_S^R - \mathbf{G}_S^A) + (\mathbf{\Gamma}_L - \mathbf{\Gamma}_R) \mathbf{G}_S^<]. \quad (\text{S20})$$

This formula applies to a general many-body Hamiltonian and Lindbladian. It can be seen that all the information about dissipation is contained in the Green's function \mathbf{G}_S . In the absence of dissipation, Eq. (S20) reduces to the Meir-Wingreen formula [S4]. By multiplying $\omega - \mathbf{X}$ from the left of $\mathbf{G}_S^< (\mathbf{G}_S^>)$ in Eq. (S17) and using the identities in Eq. (S12), we obtain

$$\begin{aligned} \mathbf{G}_S^< &= \mathbf{G}_S^R (\Sigma_{SL}^R \mathbf{g}_L^< \Sigma_{LS}^A + \Sigma_{SR}^R \mathbf{g}_R^< \Sigma_{RS}^A + 2i\mathbf{Q}) \mathbf{G}_S^A, \\ \mathbf{G}_S^> &= \mathbf{G}_S^R (\Sigma_{SL}^R \mathbf{g}_L^> \Sigma_{LS}^A + \Sigma_{SR}^R \mathbf{g}_R^> \Sigma_{RS}^A - 2i\mathbf{P}) \mathbf{G}_S^A, \end{aligned} \quad (\text{S21})$$

where we assume no dissipation in the leads, such that $\Sigma_{SL}^> = \Sigma_{SR}^> = 0$. Then, noting that $\Sigma_{SL(R)}^R \mathbf{g}_{L(R)}^< \Sigma_{L(R)S}^A = i f_{L(R)} \mathbf{\Gamma}_{L(R)}$ and $\Sigma_{SL(R)}^R \mathbf{g}_{L(R)}^> \Sigma_{L(R)S}^A = i (f_{L(R)} - 1) \mathbf{\Gamma}_{L(R)}$, we finally obtain

$$\begin{aligned} \mathbf{G}_S^< &= i \mathbf{G}_S^R (f_L \mathbf{\Gamma}_L + f_R \mathbf{\Gamma}_R + 2\mathbf{Q}) \mathbf{G}_S^A, \\ \mathbf{G}_S^> &= i \mathbf{G}_S^R (f_L \mathbf{\Gamma}_L + f_R \mathbf{\Gamma}_R - \mathbf{\Gamma}_L - \mathbf{\Gamma}_R - 2\mathbf{P}) \mathbf{G}_S^A. \end{aligned} \quad (\text{S22})$$

where $\mathbf{G}_S^{\mathcal{R}} = (\mathbf{G}_S^{\mathcal{A}})^\dagger = [(\mathbf{g}_S^{\mathcal{R}})^{-1} - \tilde{\Sigma}_L^{\mathcal{R}} - \tilde{\Sigma}_R^{\mathcal{R}}]^{-1}$, and $(\mathbf{g}_S^{\mathcal{R}})^{-1} = \omega - \mathbf{h}_S + i\mathbf{P} + i\mathbf{Q}$. Substituting Eq. (S22) into Eq. (S20) and using the identity $\mathbf{G}_S^{\mathcal{R}} - \mathbf{G}_S^{\mathcal{A}} = \mathbf{G}_S^> - \mathbf{G}_S^<$, the current can be written in a simple form

$$J^\lambda = J_{LR}^\lambda + J_{LS}^\lambda - J_{RS}^\lambda, \quad (\text{S23})$$

with

$$\begin{aligned} J_{LR}^\lambda &= \int \frac{d\omega}{2h} (f_L - f_R) \omega^\lambda \text{Tr}[\Gamma_L \mathbf{G}_S^{\mathcal{R}} \Gamma_R \mathbf{G}_S^{\mathcal{A}} + \Gamma_R \mathbf{G}_S^{\mathcal{R}} \Gamma_L \mathbf{G}_S^{\mathcal{A}}], \\ J_{LS}^\lambda &= \int \frac{d\omega}{h} f_L \omega^\lambda \text{Tr}[\Gamma_L \mathbf{G}_S^{\mathcal{R}} \mathbf{P} \mathbf{G}_S^{\mathcal{A}}] + \int \frac{d\omega}{h} (f_L - 1) \omega^\lambda \text{Tr}[\Gamma_L \mathbf{G}_S^{\mathcal{R}} \mathbf{Q} \mathbf{G}_S^{\mathcal{A}}], \\ J_{RS}^\lambda &= \int \frac{d\omega}{h} f_R \omega^\lambda \text{Tr}[\Gamma_R \mathbf{G}_S^{\mathcal{R}} \mathbf{P} \mathbf{G}_S^{\mathcal{A}}] + \int \frac{d\omega}{h} (f_R - 1) \omega^\lambda \text{Tr}[\Gamma_R \mathbf{G}_S^{\mathcal{R}} \mathbf{Q} \mathbf{G}_S^{\mathcal{A}}]. \end{aligned} \quad (\text{S24})$$

Here, the Landauer term J_{LR}^λ describes the current flow from the left lead to the right lead directly, and $J_{LS}^\lambda - J_{RS}^\lambda$ represents the current flow from the left lead to the right lead through the reservoirs.

Though Eq. (S23) gives clear physical origin for the steady-state current, it is more convenient to separate the current into

$$J^\lambda = J_0^\lambda + \delta J_1^\lambda, \quad (\text{S25})$$

where the reference current J_0^λ represents the net current if both leads are at the same chemical potential and temperature. The response current δJ_1^λ captures the change in current induced by a chemical potential and temperature gradient. Suppose the chemical potential and temperature gradient are applied to the left lead, i.e., $\mu_R = \mu$, $T_R = T$, $f_R = f$, and $\mu_L = \mu_R + \delta\mu$, $T_L = T_R + \delta T$, $f_L = f_R + \delta f$. Then, we can derive

$$J_0^\lambda = \int \frac{d\omega}{h} \omega^\lambda f(\omega) \tau_{0,l}(\omega) + \int \frac{d\omega}{h} \omega^\lambda (f - 1) \tau_{0,g}(\omega), \quad \delta J_1^\lambda = \int \frac{d\omega}{h} \omega^\lambda \delta f(\omega) \tau_1(\omega), \quad (\text{S26})$$

where the transmission function from the loss channels is $\tau_{0,l}(\omega) = \text{Tr}[(\Gamma_L - \Gamma_R) \mathbf{G}_S^{\mathcal{R}} \mathbf{P} \mathbf{G}_S^{\mathcal{A}}]$, the transmission function from the gain channels is $\tau_{0,g}(\omega) = \text{Tr}[(\Gamma_L - \Gamma_R) \mathbf{G}_S^{\mathcal{R}} \mathbf{Q} \mathbf{G}_S^{\mathcal{A}}]$, and the transmission function τ_1 is $\tau_1(\omega) = \text{Tr}[\frac{1}{2} \Gamma_L \mathbf{G}_S^{\mathcal{R}} \Gamma_R \mathbf{G}_S^{\mathcal{A}} + \frac{1}{2} \Gamma_R \mathbf{G}_S^{\mathcal{R}} \Gamma_L \mathbf{G}_S^{\mathcal{A}} + \Gamma_L \mathbf{G}_S^{\mathcal{R}} (\mathbf{P} + \mathbf{Q}) \mathbf{G}_S^{\mathcal{A}}]$.

IV. Effect of inversion symmetry in gain or loss terms on the current: a two-site example

In the main text, we have mentioned that when there is no chemical potential or temperature difference between the leads, the breaking of inversion symmetry in the gain or loss terms, or in the system, can lead to the generation of current. Consider a two-site example with Hamiltonian $H_S = -(c_1^\dagger c_2 + c_2^\dagger c_1)$. The local on-site monitoring is described by Lindblad operators $L_1 = \sqrt{\gamma_1} c_1$ and $L_2 = \sqrt{\gamma_2} c_2$. The leads self-energies $(\tilde{\Sigma}_L^{\mathcal{R}})_{11} = (\tilde{\Sigma}_R^{\mathcal{R}})_{NN} = -\frac{i\Gamma}{2}$ are constants in the wide-band limit. The particle current in Eq. (S25) is $J_0^0 = \Gamma \int \frac{d\omega}{h} f(\omega) \tau_{0,l}(\omega)$ with

$$\tau_{0,l}(\omega) = \frac{\gamma_1 (|\omega + i\gamma_2 + \frac{i\Gamma}{2}|^2 - 1) - \gamma_2 (|\omega + i\gamma_1 + \frac{i\Gamma}{2}|^2 - 1)}{|\omega + i\gamma_1 + \frac{i\Gamma}{2}| (\omega + i\gamma_2 + \frac{i\Gamma}{2}) - 1|^2}. \quad (\text{S27})$$

Now consider the situation where the monitoring strength is very small, i.e., $\gamma_1, \gamma_2 \ll \omega$. Then, Eq. (S27) can be simplified to

$$\tau_{0,l}(\omega) \approx (\gamma_1 - \gamma_2) \frac{|\omega + \frac{i\Gamma}{2}|^2 - 1}{|(\omega + \frac{i\Gamma}{2})^2 - 1|^2}. \quad (\text{S28})$$

As a result, $J_0^0 \propto \gamma_1 - \gamma_2$ for weak γ_1 and γ_2 , and in the presence of inversion symmetry, where $\gamma_1 = \gamma_2$, the current J_0^0 vanishes, as shown in Fig. 2(b2) in the main text.

Numerically, we checked that the results can be generalized to the model with more sites. Fig. S1 shows an example with five sites. Similar to the $N = 2$ case, the current J_0^0 is proportional to γ_0 for small monitoring at the second or fourth site. However, the current vanishes when measuring at the second and fourth sites due to inversion symmetry. It can be verified that adding gain or loss terms at more sites leads to the same conclusion: the presence or absence of inversion symmetry causes the current to vanish or emerge.

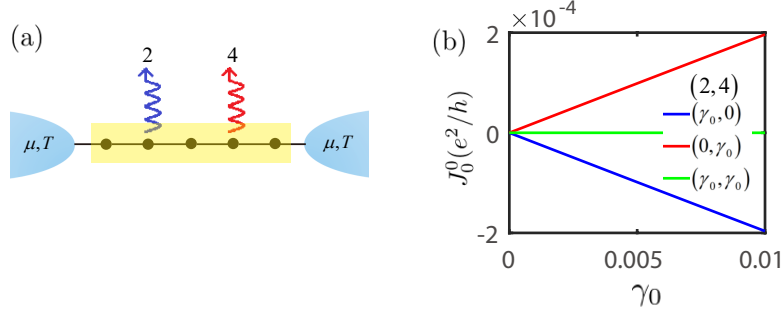


Figure S1: (a) Scheme of a five-site system with local monitoring. (b) The current J_0^0 as a function of monitoring strength γ_0 . The blue and red lines represent monitoring at the second and fourth site, respectively; the green line corresponds to monitoring at the second and fourth sites situationally.

V. Disorder-induced current generation

In this section, we use a two-site model as an example to demonstrate the relationship between the sample average of the square of the disorder-induced current and the disorder strength V . The Hamiltonian of the model is $H_S = -(c_1^\dagger c_2 + h.c.) + \sum_{j=1}^2 V_j c_j^\dagger c_j$, where the potential V_j is randomly distributed in $[-V, V]$. The on-site loss terms are $L_j = \sqrt{\gamma} c_j$, with $j = 1, 2$, and exhibit inversion symmetry. The transmission function can be derived

$$\tau_{0,l}(\omega) = \gamma \frac{\bar{V}_2^2 - \bar{V}_1^2}{(\bar{V}_1 \bar{V}_2 - \bar{\gamma}^2 - 1)^2 + \bar{\gamma}^2 (\bar{V}_1 + \bar{V}_2)^2}, \quad (\text{S29})$$

where the shifted potentials $\bar{V}_1 = \omega - V_1$ and $\bar{V}_2 = \omega - V_2$ are randomly distributed in $[\omega - V, \omega + V]$, and $\bar{\gamma} = \gamma + \frac{\Gamma}{2}$. In the weak disorder and weak dissipation limit, where $\bar{V}, \bar{\gamma} \ll 1$, the transmission function can be approximated by $\tau_{0,l}(\omega) \sim \gamma [(\omega - V_2)^2 - (\omega - V_1)^2]$. The disorder average of $\tau_{0,l}^2(\omega)$ is

$$\langle \tau_{0,l}^2(\omega) \rangle \sim \frac{\gamma^2}{4V^2} \int_{-V}^V [(\omega - V_2)^2 - (\omega - V_1)^2]^2 dV_1 dV_2 = \frac{8}{45} \gamma^2 V^2 (15\omega^2 + V^2). \quad (\text{S30})$$

It is easy to see that $\langle \tau_{0,l}^2(\omega) \rangle \sim V^4$ for $\omega = 0$ and $\langle \tau_{0,l}^2(\omega) \rangle \sim V^2$ for $\omega \neq 0$. The sample average of the square of the current can then be estimated by

$$\langle (J_0^0)^2 \rangle \sim \Gamma^2 \int \frac{d\omega}{h} f^2(\omega) \langle \tau_{0,l}^2(\omega) \rangle \sim \gamma^2 \Gamma^2 V^2. \quad (\text{S31})$$

In the integral, we consider the facts that all the frequencies that $f(\omega) \neq 0$ contribute to the fluctuation of the current. Hence, the scaling of $\langle (J_0^0)^2 \rangle$ with respect to V is dominated by $\omega \neq 0$, and then we obtain the scaling $\langle (J_0^0)^2 \rangle \sim V^2$. It can be shown numerically that this scaling relation holds for large system size N (see Fig. 2(d) in the main text).

VI. Response current and the Wiedemann-Franz law

In this section, we focus on the response current δJ_1^λ . In the presence of chemical potential and temperature gradients, the change in currents can be written as

$$\begin{pmatrix} \delta J_1^0 \\ \delta J_1^Q \end{pmatrix} = \begin{pmatrix} L_{11} & L_{12} \\ L_{21} & L_{22} \end{pmatrix} \begin{pmatrix} \frac{\delta \mu}{T} \\ \frac{\delta T}{T^2} \end{pmatrix}, \quad (\text{S32})$$

where $\delta J_1^Q = \delta J_1^0 - \mu_L \delta J_1^1$, and \mathbf{L} is the Onsager matrix [S5, S6]. Then, the electrical conductance G , the thermal conductance K , and the Seebeck factor (or thermopower) S can be expressed as

$$G = \frac{e^2}{T} L_{11}, \quad K = \frac{1}{T^2} \frac{\det |\mathbf{L}|}{L_{11}}, \quad S = \frac{1}{eT} \frac{L_{12}}{L_{11}}. \quad (\text{S33})$$

where Δ_{ij} is the determinant of the submatrix of $(\mathbf{G}_S^{\mathcal{R}})^{-1}$ from i -th row and i -th column to j -th row and j -th column [S8], which is determined by the iterative equations:

$$\begin{aligned} \begin{pmatrix} \Delta_{1,j} \\ \Delta_{1,j-1} \end{pmatrix} &= \begin{pmatrix} \omega - \tilde{X}_{j,j} & -X_{j-1,j}X_{j,j-1} \\ 1 & 0 \end{pmatrix} \begin{pmatrix} \Delta_{1,j-1} \\ \Delta_{1,j-2} \end{pmatrix} \\ \begin{pmatrix} \Delta_{j,N} \\ \Delta_{j+1,N} \end{pmatrix} &= \begin{pmatrix} \omega - \tilde{X}_{j,j} & -X_{j,j+1}X_{j+1,j} \\ 1 & 0 \end{pmatrix} \begin{pmatrix} \Delta_{j+1,N} \\ \Delta_{j+2,N} \end{pmatrix} \end{aligned} \quad (\text{S41})$$

where $\Delta_{1,0} = 1$, $\Delta_{1,1} = \omega - \tilde{X}_{1,1}$, $\Delta_{N,N} = \omega - \tilde{X}_{N,N}$ and $\Delta_{N+1,N} = 1$, and $\tilde{X}_{1,1} = X_{1,1} + (\tilde{\Sigma}_L^{\mathcal{R}})_{11}$, $\tilde{X}_{j,j} = X_{j,j}$ for $j = 2, 3, \dots, N-1$, $X_{N,N} = X_{N,N} + (\tilde{\Sigma}_R^{\mathcal{R}})_{NN}$. Defining the transfer matrix

$$\bar{T}_j = \begin{pmatrix} \omega - X_{jj} & -X_{j-1,j}X_{j,j-1} \\ 1 & 0 \end{pmatrix}, \quad \tilde{T}_j = \begin{pmatrix} \omega - X_{jj} & -X_{j,j+1}X_{j+1,j} \\ 1 & 0 \end{pmatrix}. \quad (\text{S42})$$

Eq. (S42) can be rewritten as

$$\begin{cases} \begin{pmatrix} \Delta_{1,j} \\ \Delta_{1,j-1} \end{pmatrix} = \bar{T}_j \bar{T}_{j-1} \cdots \bar{T}_1 \begin{pmatrix} 1 \\ \frac{(\tilde{\Sigma}_L^{\mathcal{R}})_{11}}{X_{0,1}X_{1,0}} \end{pmatrix}, & 1 \leq j < N, \\ \begin{pmatrix} \Delta_{1,N} \\ \Delta_{1,N-1} \end{pmatrix} = \begin{pmatrix} 1 & -(\tilde{\Sigma}_R^{\mathcal{R}})_{NN} \\ 0 & 1 \end{pmatrix} \bar{T}_N \bar{T}_{N-1} \cdots \bar{T}_1 \begin{pmatrix} 1 \\ \frac{(\tilde{\Sigma}_L^{\mathcal{R}})_{11}}{X_{0,1}X_{1,0}} \end{pmatrix}, & j = N. \end{cases} \quad (\text{S43})$$

$$\begin{cases} \begin{pmatrix} \Delta_{1,N} \\ \Delta_{2,N} \end{pmatrix} = \begin{pmatrix} 1 & -(\tilde{\Sigma}_L^{\mathcal{R}})_{11} \\ 0 & 1 \end{pmatrix} \tilde{T}_1 \tilde{T}_2 \cdots \tilde{T}_N \begin{pmatrix} 1 \\ \frac{(\tilde{\Sigma}_R^{\mathcal{R}})_{NN}}{X_{N,N+1}X_{N+1,N}} \end{pmatrix}, & j = 1, \\ \begin{pmatrix} \Delta_{j,N} \\ \Delta_{j+1,N} \end{pmatrix} = \tilde{T}_j \tilde{T}_{j+1} \cdots \tilde{T}_N \begin{pmatrix} 1 \\ \frac{(\tilde{\Sigma}_R^{\mathcal{R}})_{NN}}{X_{N,N+1}X_{N+1,N}} \end{pmatrix}, & 1 < j \leq N. \end{cases}$$

Here, for convenience, we define $X_{N,N+1} = X_{N,1}$, $X_{N+1,N} = X_{1,N}$, $X_{1,0} = X_{1,N}$ and $X_{0,1} = X_{N,1}$. Substituting Eq. (S40) into Eq. (S38), we obtain

$$\begin{aligned} \tau_{0,l}(\omega) &= 2\gamma_- \Gamma \sum_{j=1}^N [(-t_S - \gamma_-)^{2N-2j} - (-t_S + \gamma_-)^{2N-2j}] \frac{|\Delta_{1,j-1}|^2}{|\Delta_{1,N}|^2} \\ &\quad + 2\gamma_- \Gamma \sum_{j=1}^{N-1} [(-t_S - \gamma_-)^{2N-2j-1} + (-t_S + \gamma_-)^{2N-2j-1}] \text{Im} \frac{\Delta_{1,j} \Delta_{1,j-1}^*}{|\Delta_{1,N}|^2}. \end{aligned} \quad (\text{S44})$$

The transfer matrix (S42) becomes

$$\bar{T} = \tilde{T} = \begin{pmatrix} \omega + 2i\gamma_- & \gamma_-^2 - t_S^2 \\ 1 & 0 \end{pmatrix}. \quad (\text{S45})$$

The eigenvalues are $\lambda_{\pm} = \frac{\omega + 2i\gamma_- \pm \Delta}{2}$, with $\Delta = \sqrt{\omega^2 - 4t^2 + 4i\omega\gamma_-}$. From Eq. (S43), we get

$$\begin{aligned} \Delta_{1,j} &= \frac{1}{\Delta} (s_{j+1} + \frac{i\Gamma}{2} s_j), \quad 1 \leq j < N, \\ \Delta_{1,N} &= \frac{1}{\Delta} [s_{N+1} + i\Gamma s_N - \frac{\Gamma^2}{4} s_{N-1}] \quad j = N, \end{aligned} \quad (\text{S46})$$

where $s_j = \lambda_+^j - \lambda_-^j$.

We consider the special case $t_S = -\gamma_-$ and the low-energy limit $\omega \ll |t_S|, \gamma_-$. Up to leading order, $\lambda_+ = 0$ and $\lambda_- = -(\omega + 2it)$, and the transmission function in Eq. (S44) can be simplified to

$$\tau_{0,l}(\omega) = \frac{4\gamma_- \Gamma}{|\Delta_{1,N}|^2} \sum_{j=1}^{N-1} (-2t_S)^{2N-2j-1} \text{Re} \left[\Delta_{1,j-1} (t_S \Delta_{1,j-1}^* + \frac{i}{2} \Delta_{1,j}^*) \right], \quad (\text{S47})$$

where

$$\begin{aligned}\Delta_{1,0}(t\Delta_{1,0}^* + \frac{i}{2}\Delta_{1,1}^*) &= \frac{\Gamma}{4} + \frac{i\omega}{2}, \\ \Delta_{1,j-1}(t\Delta_{1,j-1}^* + \frac{i}{2}\Delta_{1,j}^*) &= \frac{i\omega}{2}[\omega^2 + \frac{1}{4}(4t_S - \Gamma)^2] \times (\omega^2 + 4t_S^2)^{j-2}, \\ |\Delta_{1,N}|^2 &= [\omega^2 + \frac{1}{4}(4t_S - \Gamma)^2]^2 \times (\omega^2 + 4t_S^2)^{N-2}.\end{aligned}\tag{S48}$$

Substituting Eq. (S48) into Eq. (S47), we obtain

$$\tau_{0,l}(\omega) = \frac{2\gamma_-^2\Gamma^2}{[\omega^2 + \frac{1}{4}(4t_S - \Gamma)^2]^2} (1 + \frac{\omega^2}{4t_S^2})^{2-N} \sim \frac{2e^2\gamma_-^2\Gamma^2}{[\omega^2 + \frac{1}{4}(4t_S - \Gamma)^2]^2} e^{-\frac{\omega^2}{4t_S^2}N}.\tag{S49}$$

Similarly, for $t_S = \gamma_-$, we can derive

$$\tau_{0,l}(\omega) \sim -\frac{2e^2\gamma_-^2\Gamma^2}{[\omega^2 + \frac{1}{4}(4t - \Gamma)^2]^2} e^{-\frac{\omega^2}{4t_S^2}N}.\tag{S50}$$

Though Eq. (S49) and Eq. (S50) are derived for $|t_S| = |\gamma_-|$, the scaling $\tau_{0,l} \sim e^{-\omega^2 N}$ provides a good approximation for $|t_S| \geq |\gamma_-|$ based on numerical calculations. Then the current at zero temperature is

$$J_0^0 = \int_{-\infty}^{\mu} \frac{d\omega}{h} \tau_{0,l}(\omega) \sim \sqrt{\frac{\pi}{4hN}} [1 + \text{erf}(\mu\sqrt{N})],\tag{S51}$$

where $\text{erf}(x) = \frac{2}{\sqrt{\pi}} \int_0^x e^{-t^2} dt$ is the error function. The asymptotic expansion of error function is $\text{erf}(x) \sim 1 - \frac{e^{-x^2}}{\sqrt{\pi x}}$ as $x \rightarrow \infty$, and $\text{erf}(x) \sim -1 - \frac{e^{-x^2}}{\sqrt{\pi x}}$ as $x \rightarrow -\infty$. Hence, in the thermodynamic limit $N \rightarrow \infty$, we obtain $J_0^0 \sim N^{-\frac{1}{2}}$ for $\mu \geq 0$, and $J_0^0 \sim \frac{e^{-N}}{N}$ for $\mu < 0$. Therefore, the current corresponding to the skin effect decreases as the size increases and vanishes as the size tends to infinity.

* Corresponding author: wangyc3@sustech.edu.cn

- [S1] K. Yamamoto, N. Hatano, Thermodynamics of the mesoscopic thermoelectric heat engine beyond the linear-response regime, *Phys. Rev. E* **92**, 042165 (2015).
- [S2] L. M. Sieberer, M. Buchhold and S. Diehl, Keldysh field theory for driven open quantum systems, *Rep. Prog. Phys.* **79**, 096001 (2016).
- [S3] F. Thompson, A. Kamenev, Field theory of many-body Lindbladian dynamics, *Annals of Physics*, **455**, 169385 (2023).
- [S4] Y. Meir, N. S. Wingreen, Landauer formula for the current through an interacting electron region, *Phys. Rev. Lett.* **68**, 2512 (1992).
- [S5] P. N. Butcher, Thermal and electrical transport formalism for electronic microstructures with many terminals, *J. Phys.: Condens. Matter* **2**, 4869 (1990).
- [S6] C. Chiaracane, A. Purkayastha, M. T. Mitchison, and J. Goold, Dephasing-enhanced performance in quasiperiodic thermal machines, *Phys. Rev. B* **105**, 134203 (2022); C. Chiaracane, M. T. Mitchison, A. Purkayastha, G. Haack, and J. Goold, Quasiperiodic quantum heat engines with a mobility edge, *Phys. Rev. Res.* **2**, 013093 (2020).
- [S7] D. A. Lavis, B. W. Southern, The inverse of a symmetric banded toeplitz matrix, *Rep. Math. Phys.* **39**, 137 (1997).
- [S8] M. Saha, B. K. Agarwalla, M. Kulkarni, A. Purkayastha, Universal Subdiffusive Behavior at Band Edges from Transfer Matrix Exceptional Points, *Phys. Rev. Lett.* **130**, 187101 (2023).